

# **PYROSHOCK SIMULATION SYSTEMS: ARE WE CORRECTLY QUALIFYING FLIGHT HARDWARE FOR PYROSHOCK ENVIRONMENTS?**

Ali R. Kolaini, Reza Nayeri, and Dennis L. Kern  
Jet Propulsion Laboratory, California Institute of Technology  
4800 Oak Grove Drive, Pasadena, CA 91109-8099

## **ABSTRACT**

There are several methods of shock testing that are commonly used by the aerospace industry to qualify flight hardware to pyroshock environments. In some cases the shock results and in particular the shock response spectra computed from these tests were interpreted in such a way as to satisfy the testing requirements and were often considered successful for flight hardware qualification. However, close scrutiny of these acquired shock data suggest gross violation of the pyroshock qualification requirements. There are several issues, both in terms of the shock generation mechanisms and the shock signature acquisition and analysis that have led to improper qualification of flight hardware. In this paper some factors contributing to the misinterpretation of the shock data are reviewed. First, issues with the hardware fixturing and instrumentation that may lead to incorrect shock testing are discussed. Second, issues facing the shock simulation systems and pyrotechnic testing are reviewed. Finally, issues pertaining to the data acquisition and analysis are briefly discussed.

**KEYWORDS:** Pyroshock testing, shock data analysis, shock data acquisition, anti-aliasing filter, shock simulation system, instrumentation

## **INTRODUCTION**

Pyrotechnic testing using ordnance/explosive devices and shock simulation systems are commonly used to qualify flight hardware for the pyroshock environments in the aerospace industry. There are issues that still confront the community with the correct application of the available methods of testing coupled with the data acquisition and shock signature analysis. One of the critical problems is that there are no universally accepted strategies that can be used for pyrotechnic data acquisition and analysis. There are several standards but none explicitly describes the processes or procedures required to produce useful, accurate, and repeatable results. Even though the pyroshock environments rarely damage most structural members, they can cause failures in electronic boxes and small brittle structures that may be sensitive to high-frequency shock energy. The Institute of Environmental Sciences and Technology (IEST) recommends hardware pyroshock testing based on a significant number of hardware failures in flight. There are a number of documents that provide detailed information on proper pyroshock data acquisition procedures. The most complete ones are the documents published by the IEST<sup>1,2</sup>. Appendix A of Reference 2 presents a valuable summary with illustrations of more common pyroshock data acquisition problems. Other documentations with valuable information concerning pyroshock testing procedures are government standards<sup>3,4</sup> and Harris's Shock and Vibration Handbook<sup>5</sup>. Other issues related to the transducer assembly mounting are discussed in some detail in Reference 6.

Pyroshock events are commonly divided into three categories: near-field, mid-field, and far-field pyroshock, as discussed in some of these references. The major differences among these categories

are proposed by Bateman<sup>7</sup> in the IEST Pyroshock Testing Techniques recommended practices. The near-field pyroshock is close to a source, has high shock levels and frequencies and transmits as wave propagation before the energy is transferred to structural responses. The mid-field pyroshock is characterized by a combination of wave propagation and structural resonances. And finally, the far-field pyroshock is characterized as lower shock levels and lower frequency structural responses.

A variety of shock simulation systems are used to simulate pyroshock events. The descriptions and details of the available systems are summarized in a report by Davie and Bateman<sup>8</sup>. This reference discusses available pyro test simulation and pyro charge systems. The electrodynamic shaker is often used to generate pyroshock environments. Even though the shock levels and spectrum can be produced accurately, the limitations of most shakers prevent achieving the full frequency band and higher level shocks. There are several mechanical impact apparatus that are used in the aerospace industry to simulate the pyroshock environments. The pro- and cons of such systems are discussed in Reference 8 in some detail.

In the following sections issues that may contribute to improper shock testing are discussed and recommendations are provided for correctly qualifying flight hardware for shock environments and processing the acquired data.

## **INSTRUMENTATION ISSUES**

Five shock accelerometers commonly used in the aerospace community are examined and the differences in the measured shock signatures are compared. The accelerometers used in this study are Endevco 7255A-01, Endevco 2225M5A, Endevco 2255B-01, PCB 350C02, and Kistler 8742. The technical specifications for these accelerometers are given in Table 1. As noted in this table some of the accelerometers have built-in mechanical and electrical filters with resonance frequency of the sensing elements close to or higher than 100 kHz. A fixture block as depicted in Figure 1 was designed to accommodate these accelerometers without introducing significant fixturing effects. The block was mounted to the Jet Propulsion Laboratory (JPL) tunable beam shock simulation system shown in Figure 1. The tunable beam consists of a 4-inch thick beam clamped at two ends, the span of which can be changed to obtain the desired knee frequencies. The beam sits on a massive support structure anchored to several feet of concrete floor. This system is similar to Sandia National Laboratory's tunable beam system; however some modifications were made to increase its capabilities to suit most of JPL testing needs. One quarter inch square steel rods are sandwiched between the clamp plates and the beam at all interfaces with damping pads sandwiched between the beam and rods. The square rods are used to minimize the beam and clamp contacts for better calibrating the knee frequencies and pads are used to damp out the high frequency shock waves. The robustness of the system is in generating shock signatures that produce the desired knee frequencies ranging from a few hundred Hz to about 3000 Hz, with levels ranging from a few hundred peak g's to more than 40k g's, and most importantly, generating re-producible shocks. The shock is generated by accelerating a slug of mass through a barrel via a pressure accumulator. The slug of mass impacts the bottom side of the beam producing the shock signature. Some of the shock data discussed in this report was acquired using a Piranha II 32 channel system with a 100 kHz sampling rate. The data acquisition (DAQ) system consisted of a built-in analog filter that rolls off at 20 kHz. The accelerometer fixture block was mounted directly onto the tunable beam with a fastener going through the center of the block.

Table 1: Accelerometers manufacturers provided technical specifications

| Accel Type       | Measurement Range [g peak] | Resonant Freq [KHZ] | Freq Response                    | Sensitivity  | Built-in Mechanical Filter | Built-in Electrical Filter |
|------------------|----------------------------|---------------------|----------------------------------|--------------|----------------------------|----------------------------|
| Endevco 7255A-01 | 50,000                     | unknown             | +/- 3dB<br>3-10,000 Hz           | 0.1 [mV/g]   | Yes, 15 KHz                | No                         |
| Endevco 2225M5A  | ?                          | 80                  | +/- 10%<br>or 1dB<br>1-10,000 Hz | 0.025 [Pc/g] | No                         | No                         |
| Endevco 2255B-01 | 50,000                     | 300                 | +/- 1dB<br>1-20,000 Hz           | 0.1[mV/g]    | No                         | Yes                        |
| PCB 350C02       | 50,000                     | >= 100              | +/- 1dB<br>4-10,000 Hz           | 0.1[mV/g]    | Yes, 23 KHz                | Yes, 13 KHz                |
| Kistler 8742     | 50,000                     | 100                 | +/- 10%,<br>1-10,000 Hz          | 0.1[mV/g]    | No                         | No                         |



Figure 1: Image of the JPL tunable beam shock simulation system and a close-up view of the block holding five shock accelerometers.

Figures 2a and 2b show a series of shock acceleration signatures obtained from the five accelerometer types discussed above and corresponding velocity plots computed by integrating the acceleration. The shock signatures were band-pass filtered to remove the DC components and cosine tapering was applied before integrating the signals. The intended shock response spectrum (SRS) for this experiment was 6000 g's with an approximate knee frequency of 1600 Hz. The SRS is broadly defined as the peak response of a SDOF oscillator to an excitation as a function of the natural frequency of the oscillator (Reference 5, chapters 23 and 26). The SRSs shown in Figure 2c

are computed using  $Q$  of 10 for the shock signatures shown in Figures 2a. In an effort to understand the quality of the shock signatures obtained using five different types of accelerometers, the Fast Fourier Transfer (FFT) functions of these signatures were computed and are plotted in Figure 3. There are several differences when the shock time-history signatures, velocities, SRSs, and FFTs shown in Figures 2 and 3 are compared. These accelerometers captured the shock events from the same source. First, the accelerometer types Endevco 2255B01 and Endevco 2225M5 indicate very high shock levels, more than a factor of two higher than others at frequencies near 8000 Hz. Second, the Endevco 2225M5 indicates low frequency content that is outside the family of the accelerometers. The Endevco 2225M5A has been identified in the past to be a major source of problems in pyroshock data acquisition shortly after it was introduced to the market and should not be used for pyrotechnic shock testing. The velocity plots indicate the PCB accelerometer provided the best shock signature without data corruption. It is not clear from the limited testing performed using these accelerometers why Endevco 2255B-01 and PCB 350C02 have higher frequency contents than the other three do not. The resonance frequencies of the crystals suggested by the manufacturers are much higher than 8000 Hz (see Table 1).

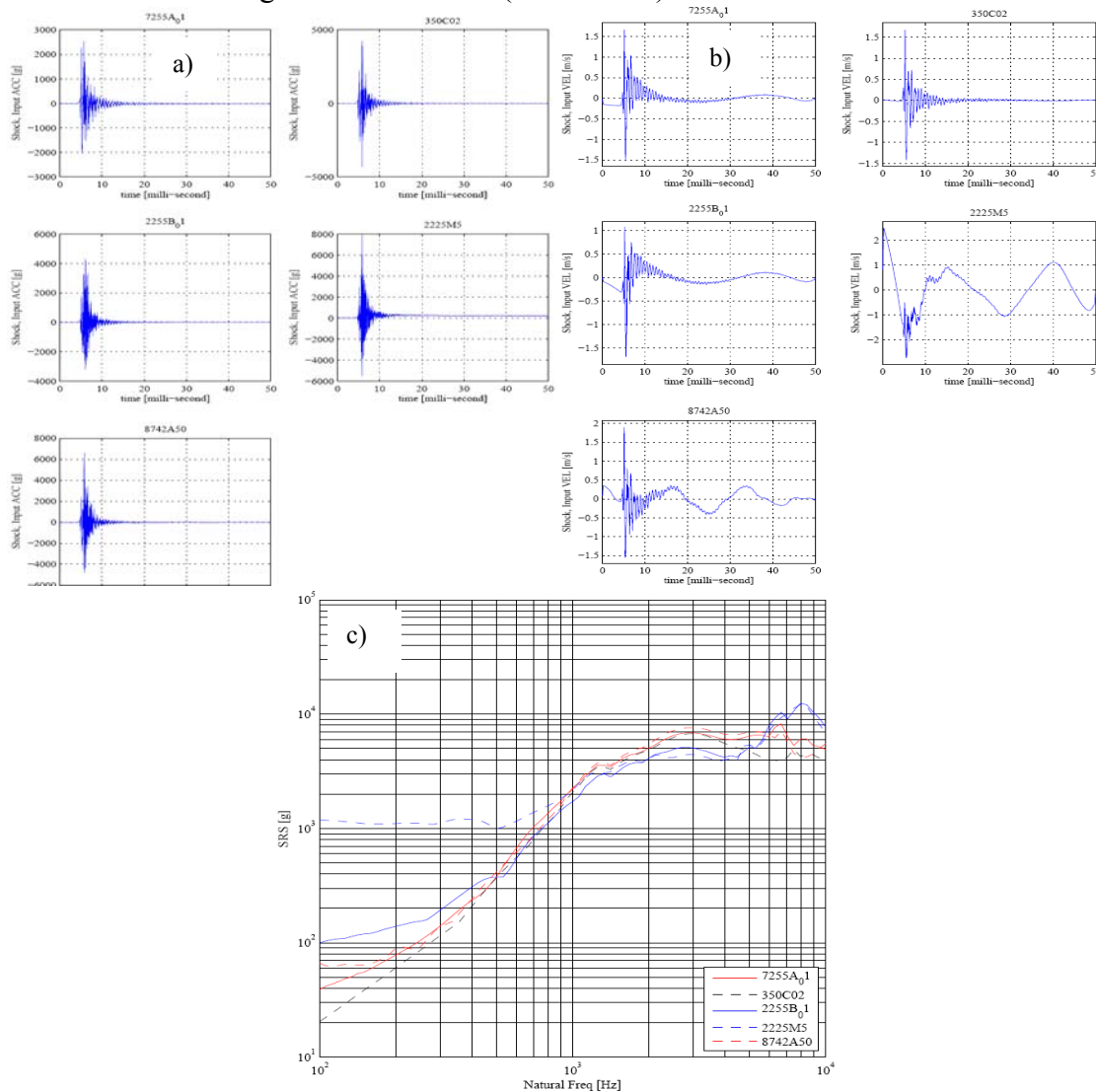


Figure 2: a) Shock acceleration signatures obtained from five accelerometers, b) the velocity plots, and c) the corresponding SRS calculated using  $Q$  of 10.

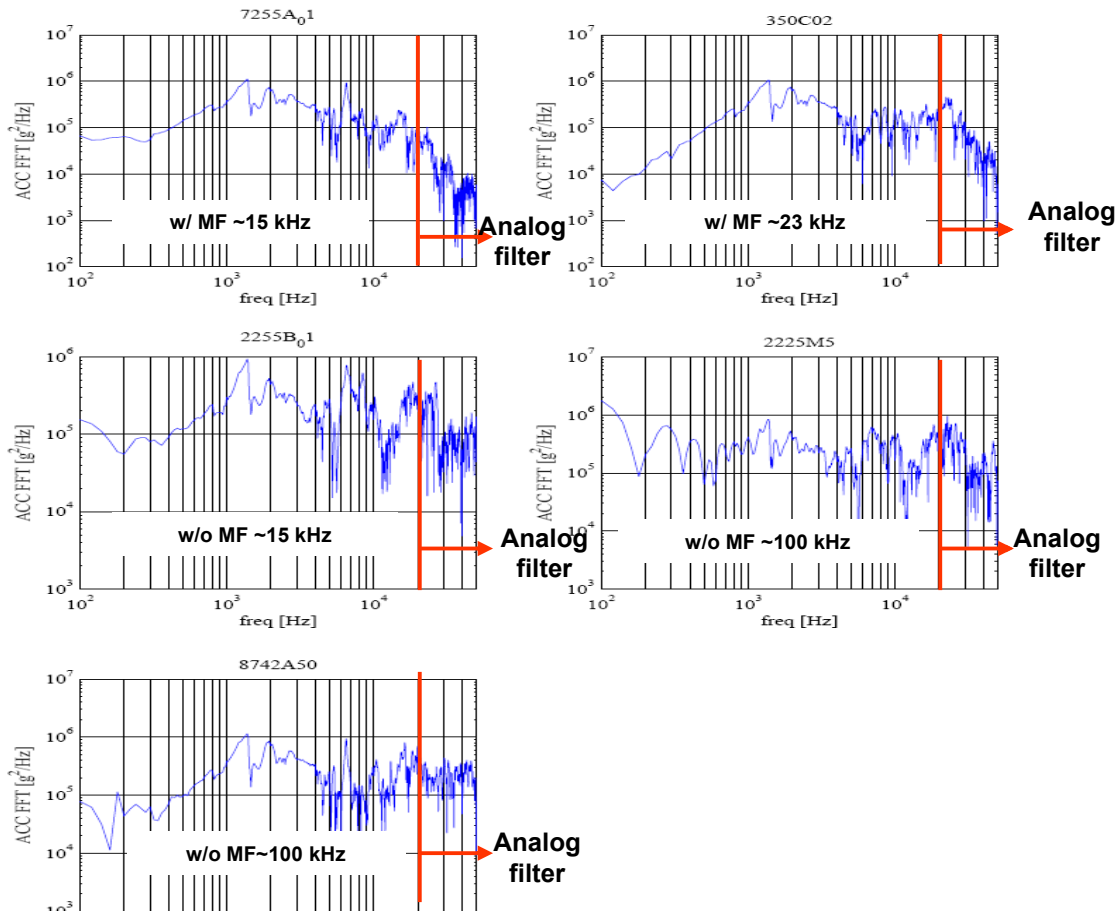


Figure 3: The FFT plots of acceleration signatures shown in Figure 2a. The built-in analog filter in the DAQ system was set at 20 kHz and the data was acquired with 100 ksamples per second.

To further examine issues with selection of the accelerometer types, consider signatures captured using two types of accelerometer from the same shock source generated by the tunable beam with levels in excess of 40k g's. Figures 4a and b indicate shock signatures obtained from Kistler 8742A50 accelerometers (two locations) and Figure 4c shows signature taken from PCB 350C02 accelerometer. The corresponding SRSs are plotted in Figure 4d. The shock signatures and the SRSs should be identical considering these accelerometers were installed on a fixture plate fastened directly to the beam with less than 2-inch spacing between the accelerometers. However, the differences in the SRSs computed using the data acquired from Kistler accelerometers and the PCB accelerometers are very clear at the lower end of the spectrum. It should be noted that the Kistler accelerometers did not have mechanical filters whereas the PCB accelerometer of the type used in this study had built-in mechanical and electrical filters as indicated in Table 1. A closer examination of the data reveals that when a high shock level is being simulated it is possible to excite the sensing elements within the accelerometers that lead to serious degradation of the quality of the shock signatures. This is shown in Figure 5a when the SRSs of the shock signatures of Figure 4 are extended to 100 kHz (half the sampling rate). The high frequency peak centered at around 50 to 60 kHz is very close to the resonance frequency of the Kistler accelerometers. In any shock testing if

the crystal element of an accelerometer that does not have a built-in mechanical filter undergoes excitation at its resonance frequency, it can lead to a nonlinear behavior impacting the quality of the data. The differences observed at the low end of the SRSs shown in Figures 4d and 5a when compared with PCB accelerometer is most likely due to this condition. The integration of the acceleration signatures (i.e. velocities) shown in Figures 5b and c clearly demonstrate the data corruption had occurred when the crystal elements of the Kistler accelerometers were forced to resonate with Figure 5d showing un-corrupted velocity signature. The recommendation is to use accelerometers that have both mechanical and electrical filters to prevent the abnormal accelerometer behavior as discussed above.

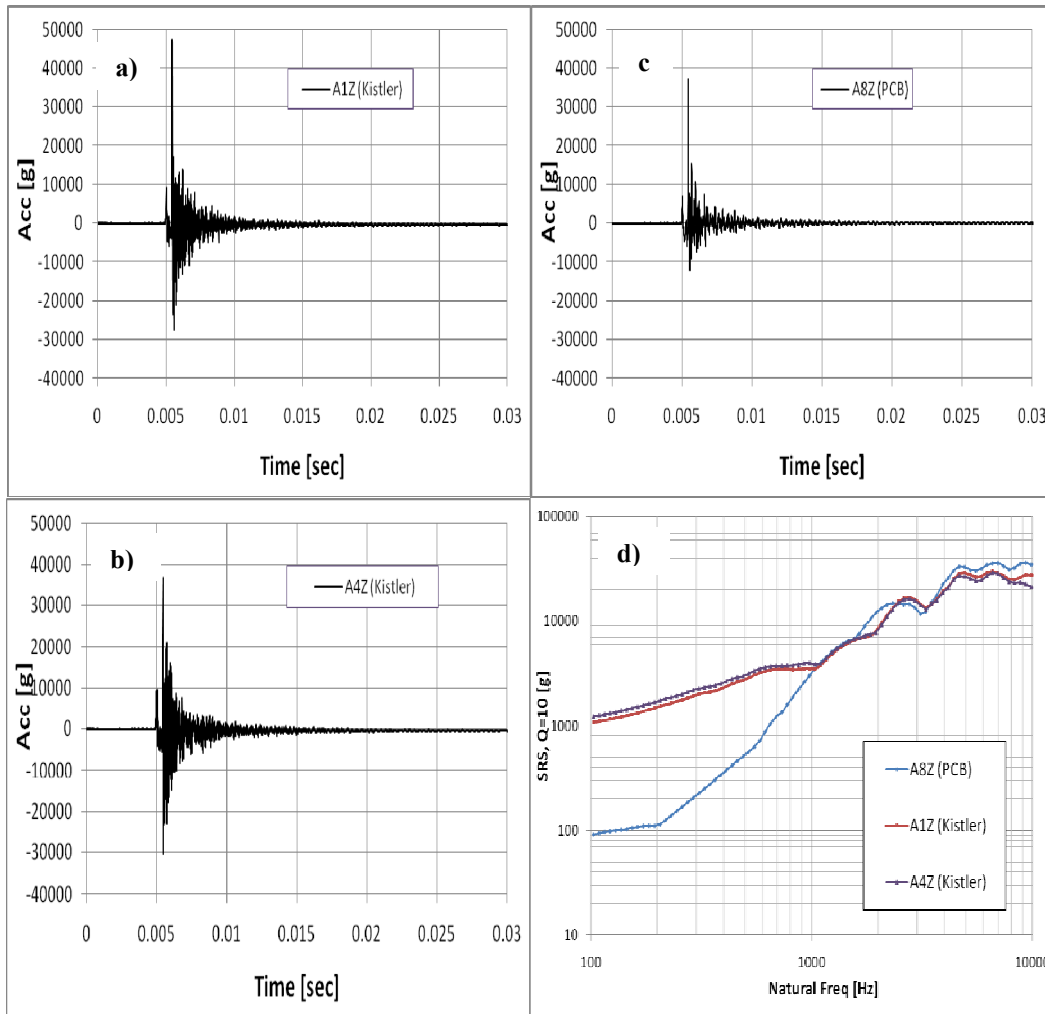


Figure 4: Shock signatures obtained from a high-shock level source generated by the tunable beam using both Kistler accelerometers (a and b), and PCB accelerometer (c). The corresponding SRSs computed using Q of 10 are shown in (d).

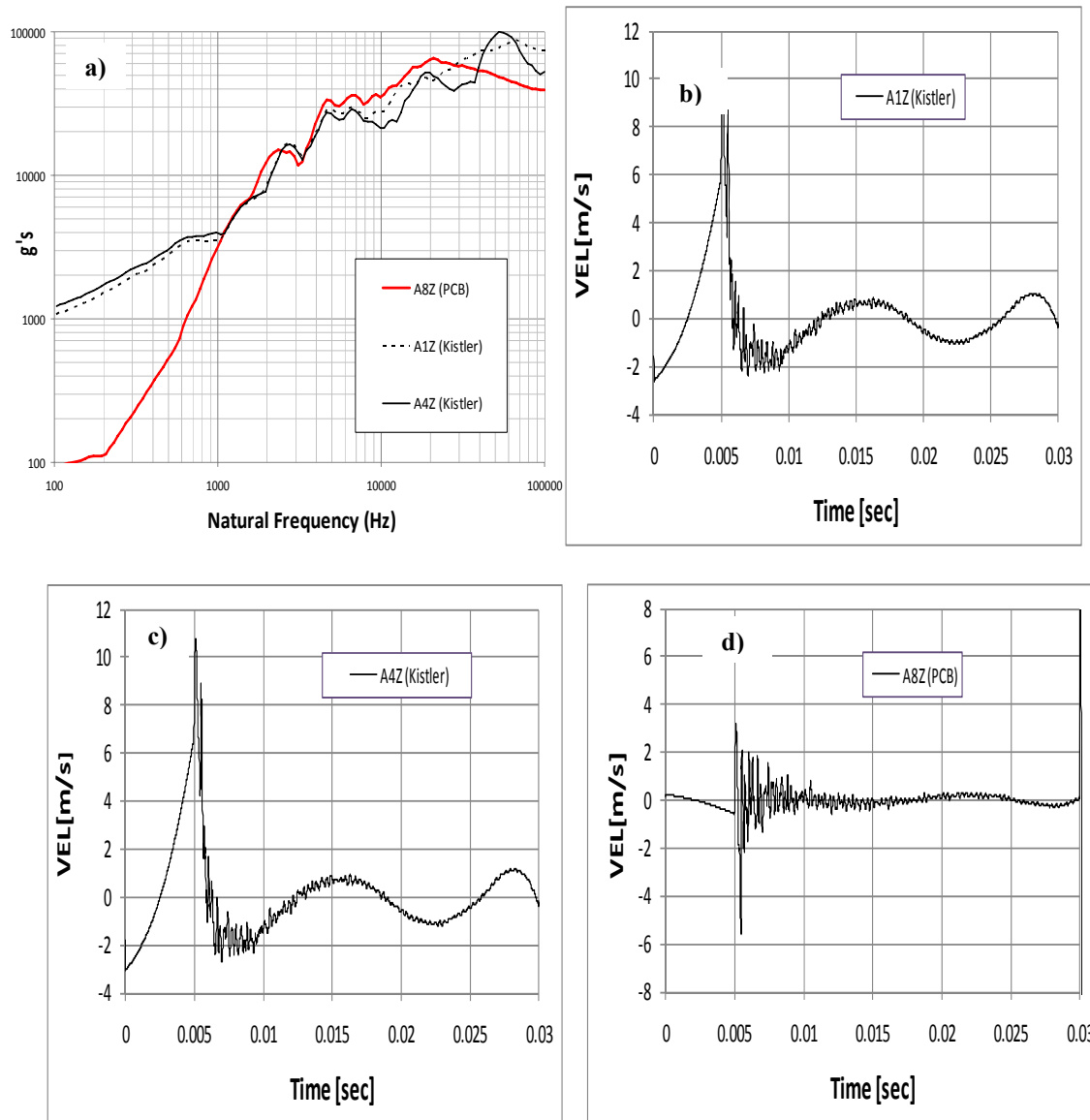


Figure 5: (a) The SRSs of Figure 4 extended to 100 kHz, which is half of the sampling rate, and (b, c, d) velocity plots.

## ANTI-ALIAS FILTER ISSUES

In some aerospace shock testing facilities, the shock data are acquired and analyzed in SRS domain without paying attention to the quality of the data. In the case of pyrotechnic tests the data acquisition and analysis of the motions produced by explosive events are very difficult to properly acquire. Recent improper data acquisition and analysis of critical flight hardware data led Smith et al<sup>9</sup> to discuss how pyrotechnic data can be acquired and analyzed to prevent the mishandling of the flight hardware qualification tests. They emphasized two important factors that may have attributed to the mishandling of the data, namely, the acquired data within the desired frequency range must be adequately protected from aliasing and energy beyond the frequency band of analysis must not be allowed to corrupt the data.

The corruption of shock data acquired with DAQ systems without an anti-aliasing filter has been discussed in communities dealing with digital signal acquisition for many years. Some pyroshock tests are still being performed without the analog anti-aliasing filter by increasing the DAQ's sampling rate to avoid the folding of the higher frequencies to within the SRS frequency range of interest. The increase in the sampling rate may not necessarily remove the data corruption as demonstrated by performing a series of shock tests using the tunable beam shock simulation system. The shock tests were performed using two separate DAQ systems. One system had a built-in analog anti-aliasing filter with a cut-off frequency of 20 kHz and the other with an option of turning the built-in analog anti-aliasing filter on/off by the user. A small block with an accelerometer stud-mounted on it was fastened to the center of the tunable beam. An attempt was made to generate a shock signature with a knee frequency of  $\sim 1600$  Hz and high frequency shock level of  $\sim 7000$  g's. A series of shock tests were performed using the DAQ systems with a rate of 100 samples per second with the anti-aliasing filters activated with a cut-off frequency of 20 kHz. The shock signatures acquired using these DAQ systems and the corresponding SRSs are plotted in Figure 6. Except for slight differences above 10 kHz, the two SRSs are identical. The FFT functions for these cases are plotted up to 50 kHz in Figure 7, with some differences noted at frequencies above 10 kHz. The steep roll-off for one of the DAQ systems is attributed to the increase in the number of poles on the analog filter. The frequency contents of the FFTs in the frequency range of 100 to 10,000 Hz are identical for the two DAQ systems.

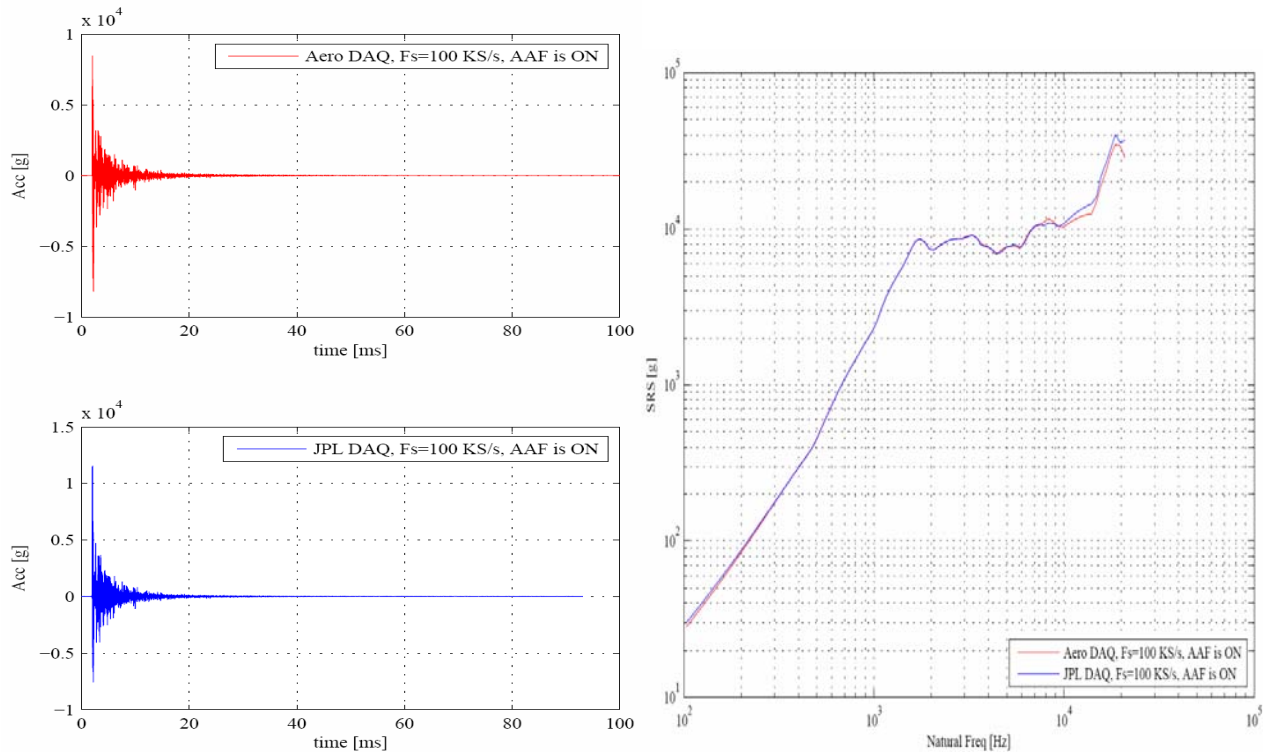


Figure 6: Shock signatures acquired using two data acquisition systems and the corresponding SRSs. The data was acquired with 100 ksamples per second using two DAQ systems that included anti-aliasing filters.

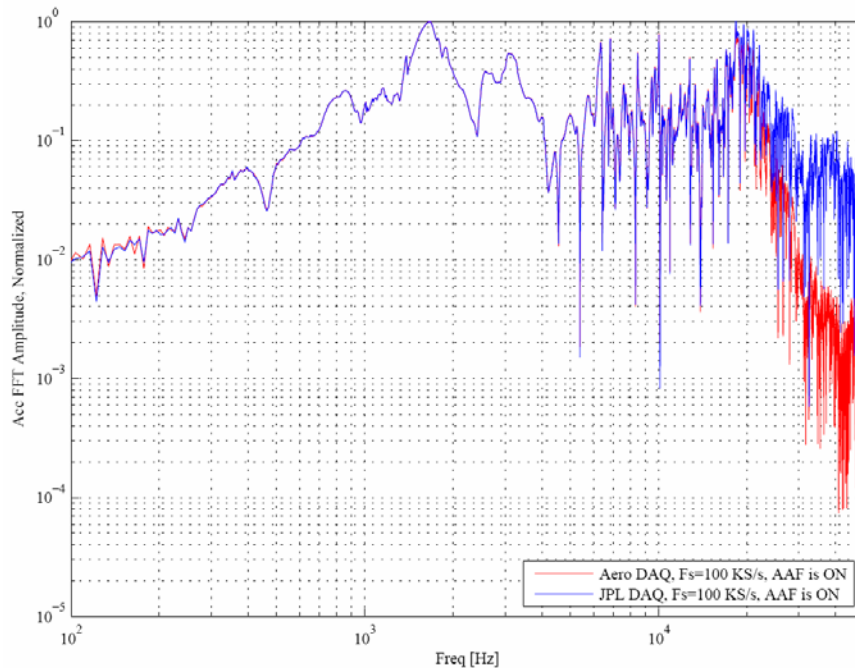


Figure 7: FFT plots of the shock signatures shown in Figure 6.

The second test was performed using the same setup with one of the DAQ systems kept at the same conditions as discussed above. However, the second DAQ system's sampling rate was increased to 1000 ksamples per second and the anti-aliasing filter was turned off. The tunable beam was calibrated to generate nominal shock levels close to 15,000 g's. The shock signature generated by this run and the data acquired using the two DAQ systems and the corresponding SRSs are shown in Figure 8. The SRS curves up to 10 kHz match very well for this case considering the fact that the anti-aliased filter was turned off on the second DAQ system. The higher sampling rate has removed the potential folding of the acceleration levels beyond 500 kHz since no significant responses have been excited pass 300 kHz as depicted in Figure 9 of the FFT functions. Using a DAQ system without an anti-aliasing filter, it is plausible to assume that the acquired data from a pyroshock test may contain frequency content with appreciable levels closer to the Nyquist frequency. In such cases the folding of the frequency could occur regardless of the sampling rate used in acquiring the data. To demonstrate that the folding of the acceleration level occurs in some cases without the anti-aliasing filter, we repeated the previous case, except we selected the sampling rate for the second DAQ system to be at 72 kHz. This frequency was selected to force the strong acceleration responses in the vicinity of 70 kHz (see Figure 9) to be folded back to the frequency range below 10 kHz. Figures 10 and 11 show the SRSs and FFTs of the shock signatures obtained for this case. It is clearly evident from Figure 10 that the differences in SRS levels are attributed to folding of the higher frequencies onto the SRS frequency range of interest, i.e. 100 Hz to 10,000 Hz.

As another example, consider the SRS level at approximately 4400 Hz shown in Figure 10 that is caused by aliasing the data at approximately 76400 Hz (Figure 9). The g level at this frequency was folded back to the lower frequency. Similar arguments hold for the other folded frequencies shown in Figures 10 and 11. This is an important factor to consider in shock testing, whether explosive devices or shock simulation systems are used to generate the shock environments. It is importance to ensure that the acquired shock data is not corrupted by aliasing caused by the DAQ system

without an anti-aliasing filter. The anti-aliased filters must be used before the analog data is converted into digital form.

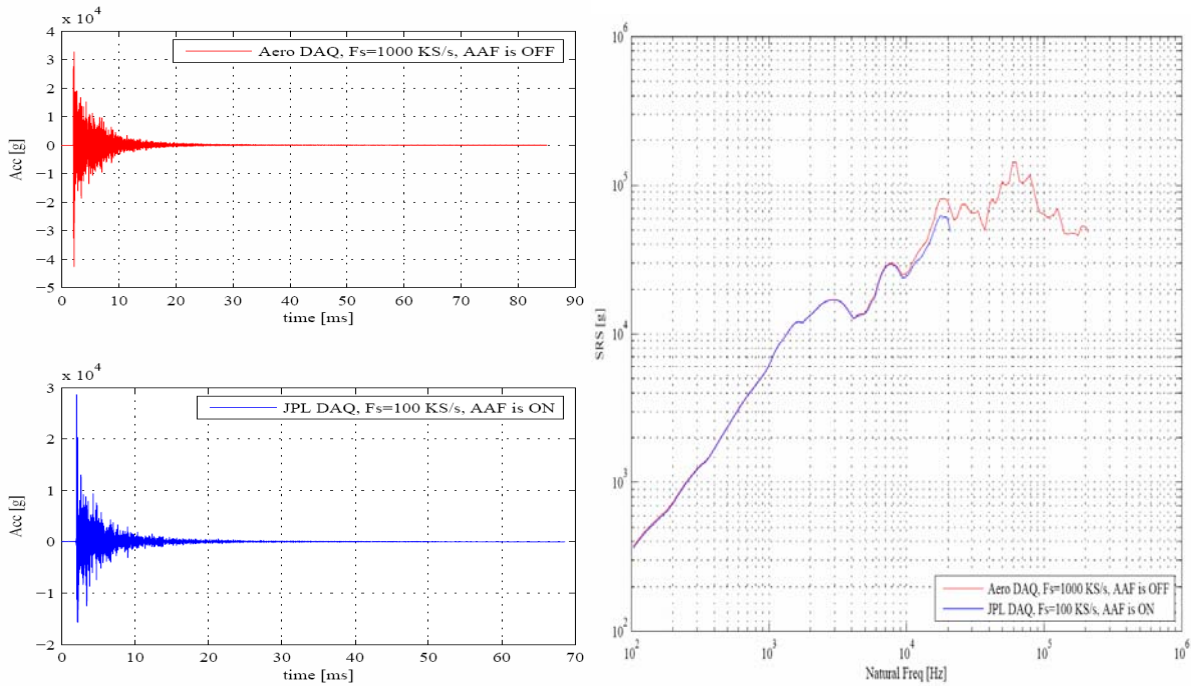


Figure 8: Shock signatures acquired using two data acquisition systems. The shock signature (blue line) was acquired using the DAQ system with 100 ksamples per second and with an anti-aliased filter turned on and the red curve was acquired using the second DAQ system with the anti-aliasing filter turned off. The corresponding SRS plots with a Q of 10 are shown.

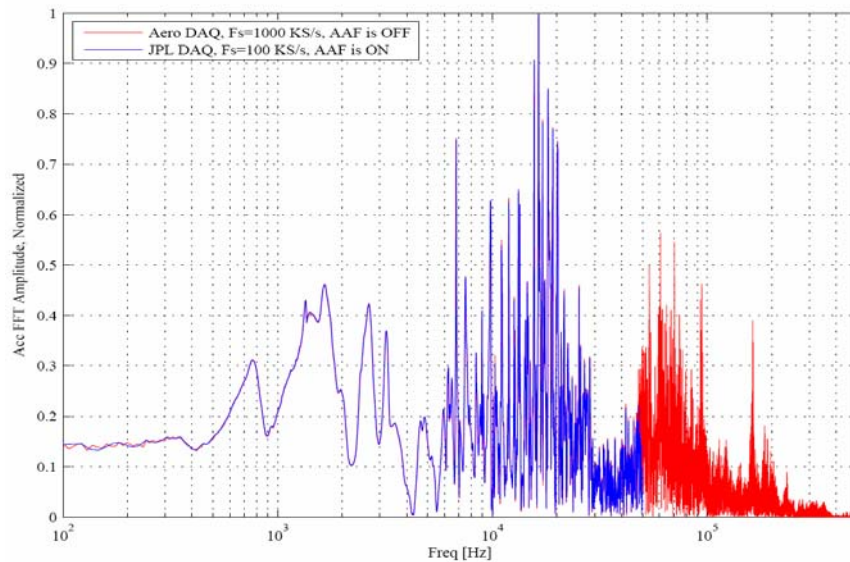


Figure 9: FFT plots of the shock signatures shown in Figure 8.

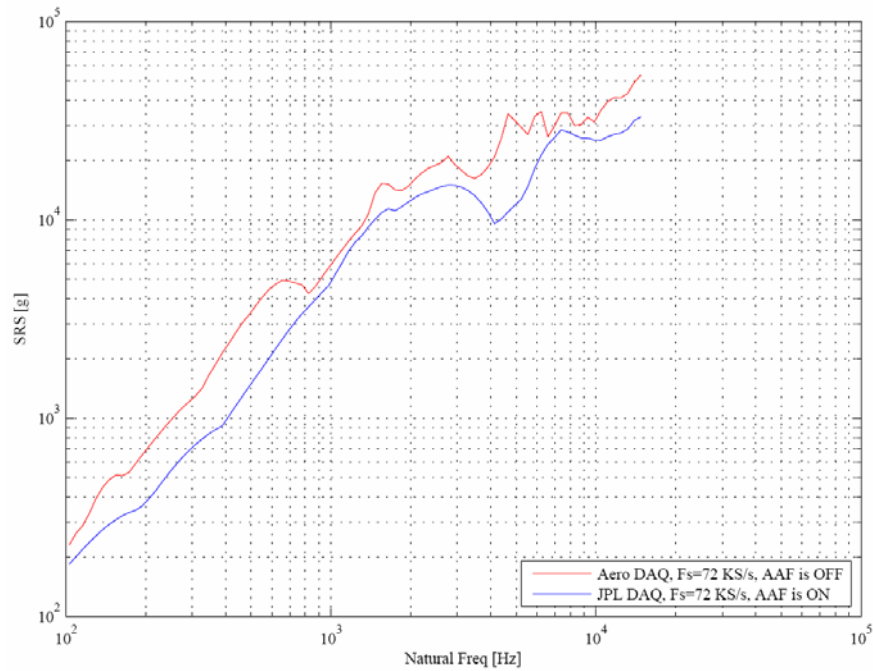


Figure 10: SRSs computed from data acquired using (a) the DAQ system with a built-in anti-aliasing filter (blue curve) and (b) using the DAQ system with no anti-aliasing filter (red curve). The observed mismatch in the SRS level is due to the data corrupted by aliasing.

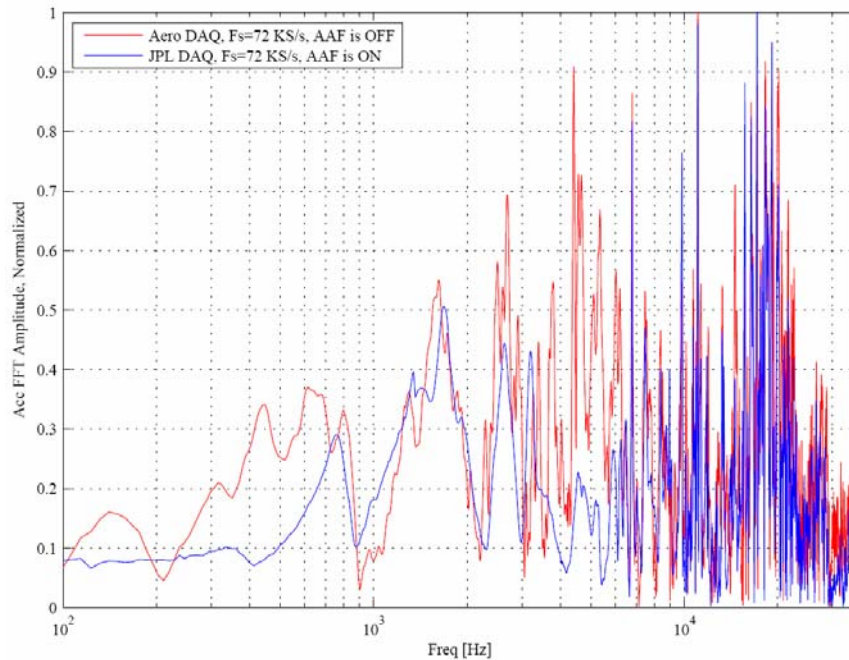


Figure 11: FFTs of the shock signatures shown in Figure 10. The blue curve is obtained from DAQ system with an anti-aliasing filter on and the red curve is a from a different DAQ system with the filter off.

## SHOCK DATA QUALITY

Selecting appropriate shock accelerometers and including anti-aliasing filters are fundamental steps in ensuring that the instrumentation and data acquant/post processing are not the cause of data corruption. Accelerometers with both mechanical and electrical filters must be selected for testing. Other factors such as test fixtures and shock simulation apparatus may also lead to invalid shock testing. In this section we present a case where the shock signatures obtained from a simulated system meet the requirements and are free of the corruption discussed in the previous section. We also present a case that has serious data quality that was attributed to test fixtures and test setups. Figure 12 indicates a case of simulated shock performed using the tunable beam. The shock signature, SRSs, and velocity plots shown in this figure are excellent for several reasons: 1) the shock duration is less than 10 msec, 2) time histories are almost symmetric, 3) the velocity computed using acceleration shows no sign of data contamination, and 4) SRSs meet the intended requirements. Figures 13 show an example that the simulated shock signature with velocity and SRSs (both min and max) lacked the quality needed to qualify the hardware for flight shock environments. In some testing centers these kinds of shock signature are often considered acceptable, especially when they only examine the maximax of the shock response spectrum.

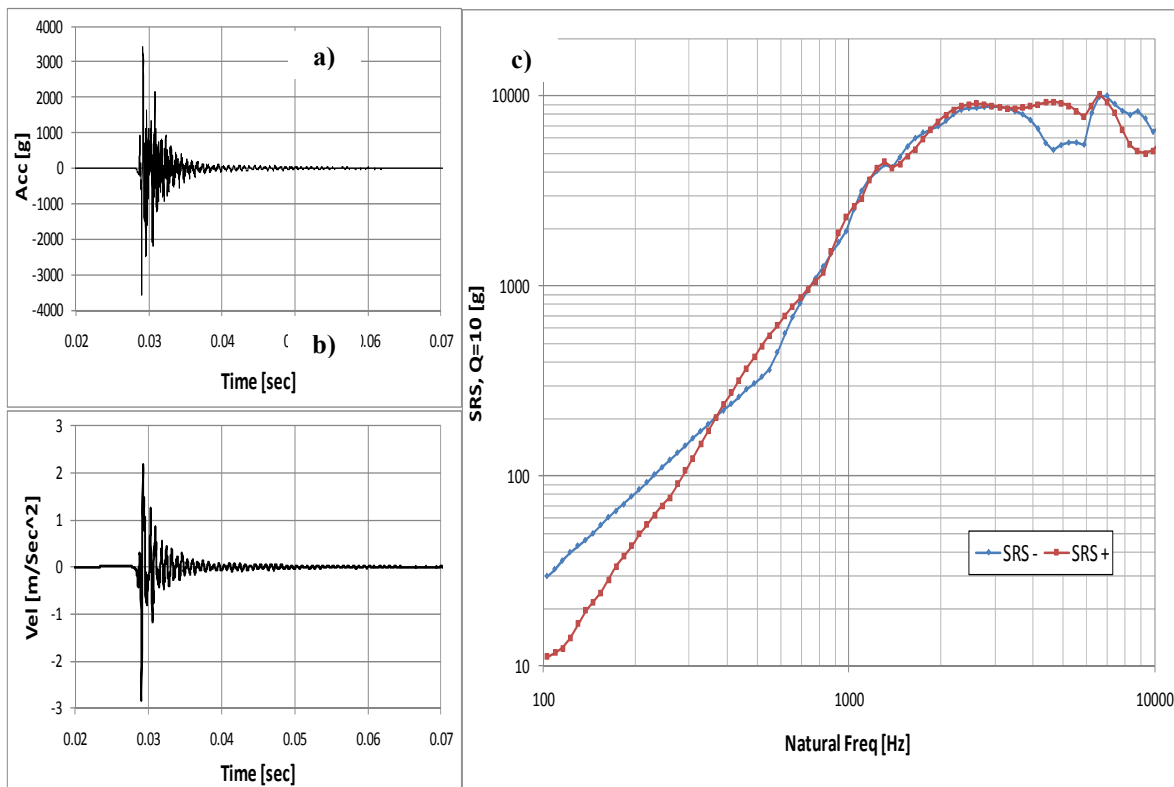


Figure 12: a) An example of a good quality shock signature, b) its corresponding velocity that is also oscillatory in nature, and c) Min/Max SRSs that are very similar.

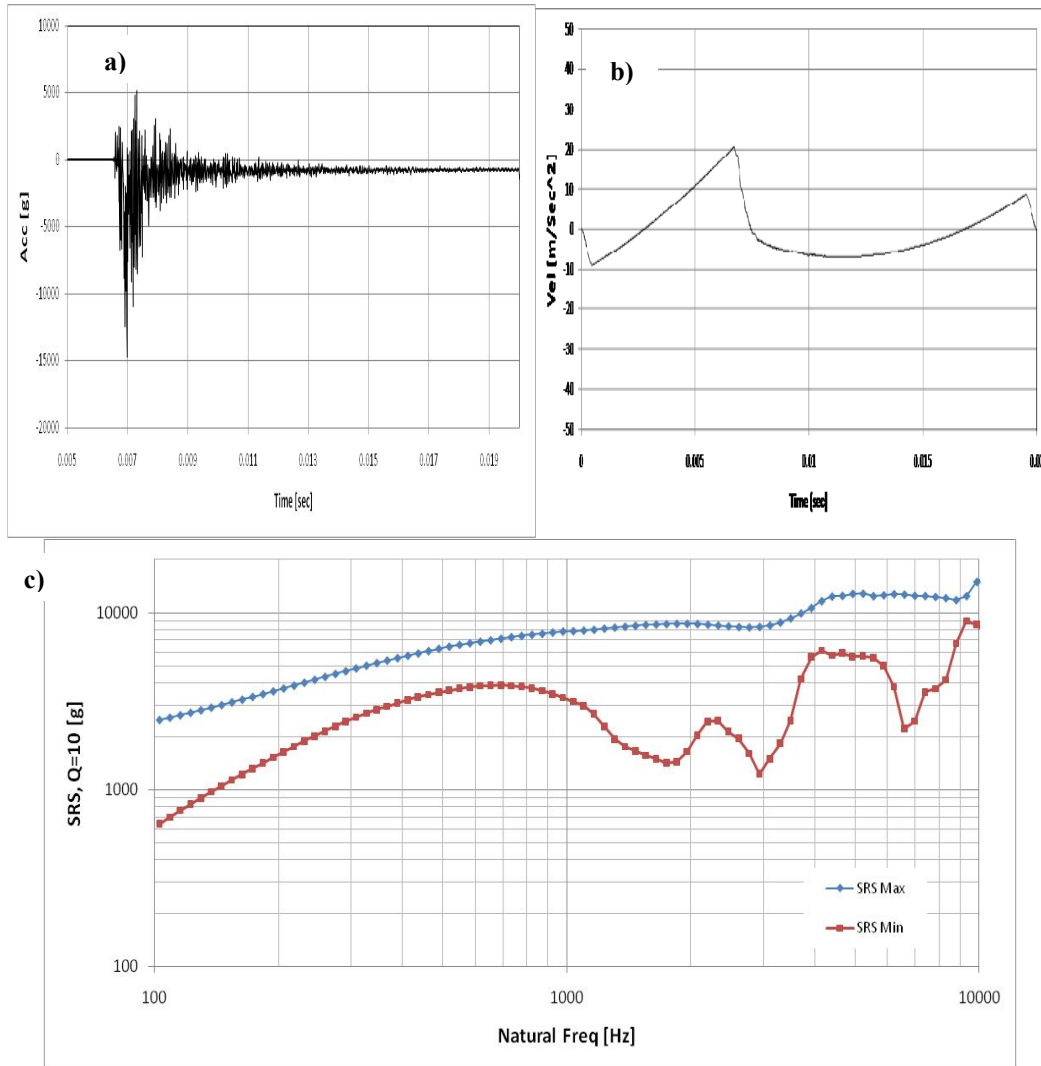


Figure 13: a) An example of a bad quality shock signature, b) the velocity signature suggests corrupted data, and c) Min/Max SRSs showing significant differences.

## CONCLUSION AND RECOMMENDATIONS

Five of the most commonly used shock accelerometers in the aerospace industry are examined in some details. Those accelerometers that lack both built-in mechanical and electrical filters may force excitation of the crystals and contaminate the data, in particular when the simulated shock environments are severe. Therefore, the proper selection of the accelerometers must be done in the preparation of the shock testing setup when flight hardware is being qualified. The absence of a built-in anti-aliasing filter may provide corrupted data. The severe aliasing and amplifier saturation can cause unrealistic shock signature not detected by the SRS plots and can only be detected if FFTs and velocities are computed. Increasing the sampling rate of the acquired data may not completely get rid of the frequency folding problem, in particular when higher shock environments are generated. Using data acquisition systems with a built-in anti-aliasing filter for any kind of digital signal data acquisition and processing is absolutely necessary.

To assess the data shock quality by examining only the maximum of the shock response spectrum is not adequate. We demonstrated that if only maximum shock spectrum is used one may not realize the degree of the contamination in the acquired data that may lead to improper flight hardware qualification. For shock tests to be performed successfully and to properly qualify flight hardware, it is recommended to examine the acceleration time history, computed velocity time history, and SRSs. In addition to these steps, we recommend FFTs of the shock signatures be computed and the folding issues be examined when a sensitive flight hardware is being tested. This may be useful for even those systems that have anti-aliasing filters in an event the filter either does not function properly and/or the cut-off frequency is not set properly. The velocity plots for pyroshock data, if the data is corrupted, may reveal a near monotonic trend in the mean velocity versus time, which is a typical result of a zero offset in the acquired acceleration data, and/or a haystack trend in the mean velocity versus time, which may be caused by amplifier saturation and/or nonlinear accelerometer behavior during the data acquisition. The correct shock data should provide velocity plots that fluctuate about the mean, as would be expected when integrating a fluctuating acceleration time history.

## ACKNOWLEDGMENT

The authors would like to thank the staff of JPL Environmental Testing Laboratory and Douglas Perry for helping conduct the shock testing discussed in this report, and the Aerospace Corporation for lending the DAQ system with on/off anti-aliasing filter capability used in this study. This research was carried out at the Jet Propulsion Laboratory, California Institute of Technology, under a contract with the National Aeronautics and Space Administration.

## REFERENCES

1. "Handbook for Dynamic Data Acquisition and Analysis", IEST-RD-DTE012.2, Appendix A, "Pyroshock Data Acquisition and Analysis", 2006.
2. "Pyroshock Testing Techniques", IEST-RP-DTE032.1, 2002 (currently undergoing revision).
3. "Pyroshock Test Criteria", NASA-STD-7003, National Aeronautics and Space Administration, Washington, D.C., May 1999 (currently undergoing revision).
4. "Pyroshock", MIL-STD-810F, Method 517, Department of Defense, Washington, D.C., January 2000 (currently undergoing revision).
5. "Concepts in Shock Data Analysis and Pyroshock testing", Chapters 23 and 26, in "Harris' Shock and Vibration Handbook", fifth edition, McGraw-Hill, NY 2002 (currently undergoing revision).
6. B. Hollowell, S. Smith, and J. Hansen, "A Close Look at the Measurement of Shock Data," 13th Aerospace Testing Seminar, 1992.
7. V.I. Bateman, "Pyroshock data acquisition – recent development using P/R and P/E accelerometers and isolators," J. Acoust. Soc. Am. Volume 111, Issue 5, pp. 2381-2381 (May 2002).
8. N.T. Davie and V.I. Bateman, "Pyroshock simulation for satellite components using a tunable resonant fixture – Phase 2," Sandia Report # SAND93-2294, April 1997.
9. S. Smith, B. Pankracij, B. Franz, and K. Ameika, "Acquiring and analyzing pyrotechnic test data – the right way," Sound and Vibration, October 2008.